Incorporation of Hydroxypyridinone Ligands into Self-Assembled Monolayers on Mesoporous Supports for Selective Actinide Sequestration

YUEHE LIN, SANDRA K. FISKUM,
WASSANA YANTASEE, HONG WU,
SHAS V. MATTIGOD,
ERICH VORPAGEL, AND
GLEN E. FRYXELL*

*Pacific Northwest National Laboratory,
Richland, Washington 99352*

KENNETH N. RAYMOND AND JIDE XU

*Department of Chemistry, University of California at Berkeley,
Berkeley, California 94720*

In this study, three isomers of hydroxypyridinones (1,2-HOPO, 3,2-HOPO, and 3,4-HOPO) were attached to self-assembled monolayers on mesoporous silica (SAMMS). The HOPO–SAMMS materials have superior solid adsorbents properties: they do not suffer from solvent swelling; their rigid, open pore structure allows rapid sorption kinetics; their extremely high surface area enables the installation of high functional density; and being silica-based, they are compatible with vitrification into a final vitreous waste form. Kinetics, equilibrium, and selectivity of the adsorptions of actinide on the HOPO–SAMMS at various pH values and in the presence of other metal cations, anions, and competing ligands are reported. Rapid sequestration of U(VI), Np(V), and Pu(IV) was observed. Very little competition from transition metal cations and common species was observed.

Introduction

DOE legacy wastes, such as those found in the underground tanks at the Hanford site, contain radioactive materials including actinide species in aqueous waste solutions. Of all the actinides, plutonium and uranium, resulting from extensive cold war production, are of the greatest concern. These radioactive materials are present at very low concentrations in millions of gallons of tank wastes (commonly 10^{-8} to 10^{-9} M). Since only the radioactive components of the waste need to be immobilized in a vitreous waste form, selective removal of the actinides could greatly reduce the volume of wastes to be subsequently vitrified or converted for long-term storage. To be effective for removing low-level actinides from tank wastes, the complexing agents must be selective for the target species among other interfering cations and/or competing ligands. Actinides tend to form insoluble hydroxides and polymeric oxide species at alkaline pH values; therefore, any general actinide separation scheme will require acidification (preferably to pH 4 or below). Thus, actinide sequestering agents must be effective in acidic environments.

New complexing agents based on hydroxypyridonates (HOPO) (*1–6*), inspired by highly selective iron-binding siderophores from bacteria, have been synthesized and evaluated for both in vivo actinide decorporation (*7–9*) and nuclear waste remediation (*10–12*). Specifically, sequestering agents based on HOPO ligands have been developed for effective mammalian Pu(IV) (*7, 8*) and U(VI) (*9*) decorporations, respectively. Hexylamide derivatives of 1,2-HOPO have been used as liquid–liquid extractants that are highly selective for Pu(IV) (*11*). However, solvent extractions are usually time- and labor-intensive and often rely on the use of toxic organic solvents, creating large volumes of secondary hazardous wastes.

The HOPO ligands have been used as solid-phase extractants by covalent attachment of the ligands onto an insoluble polymer resin for plutonium removal (*12*). Polymers have been known to suffer from solvent swelling that may slow the adsorption rate of the polymeric-based adsorbents or lead to particle attrition and the generation of fines.

Through the marriage of nanoporous ceramics (MCM-41) with self-assembled monolayer chemistry, a powerful new class of sorbent materials has been created at the Pacific Northwest National Laboratory (PNNL) (see Figure 1) (*13–28*). These self-assembled monolayers on mesoporous supports (SAMMS) material are highly efficient sorbents. Their interfacial chemistry can be fine-tuned to selectively sequester various target species, including heavy metals (*15–17*), cesium (*18*), radioiodine (*19*), actinides (*20–24*), and oxometalate anions (*25–28*).

In this study, mesoporous silica (MCM-41) was chosen as the support because its honeycomb structure with rigid, uniform wall structure (*29*) does not allow solvent swelling yet is readily decorated with ligand fields (*30, 31*). The pore dimensions are suitable for easy transport of metal ions in to and out of the pores, even after the attachment of the monolayer ligand fields. In addition, this morphology results in extremely large surface area (900–1000 m²/g) in a very compact volume, ultimately creating a very high functional density. Silica-based materials have been melted into glasses for centuries. Melting actinide-laden SAMMS should result in the organic ligand being burned off, leaving the actinide silicate encased in a glass matrix suitable for long-term storage in a deep geological repository. This disposal strategy also avoids the generation of secondary waste streams that are produced by other actinide separation processes (e.g., solvent extraction). Three HOPO ligands (1,2-HOPO, 3,2-HOPO, and 3,4-HOPO) were attached to the monolayer interface of SAMMS for the selective removal of actinides from various acidic media. The kinetics, equilibrium, and selectivity of the adsorptions of the HOPO–SAMMS materials for actinide cations in the presence of transition metal cations, anions, and competing ligands were evaluated.

Experimental Section

HOPO–SAMMS Syntheses. The methods for the syntheses of the benzyl-protected HOPO acids (1,2-HOPOBn-6-carboxylic acid, *N*-methyl-3,2-HOPOBn-4-carboxylic acid, and 2-methyl-3,4-HOPOBn-*N*-acetic acid) have been published elsewhere (*1–6, 8, 32*). The procedures for the attachment of HOPO moieties onto mesoporous silica are shown in Figure 2. The benzyl-protected HOPO acids were each dissolved in anhydrous dimethylformamide (DMF) (under dry N₂) and treated with 1.0 equiv of carbonyldiimidazole (CDI). After cessation of N₂ evolution (usually about 20 min), 1.0 equiv of freshly distilled 3-aminopropyl trimethoxysilane (APS) was added. The resulting solution was stirred at ambient tem-

* Corresponding author phone: (509)375-3856; fax: (509)375-2186; e-mail: glen.fryxell@pnl.gov.
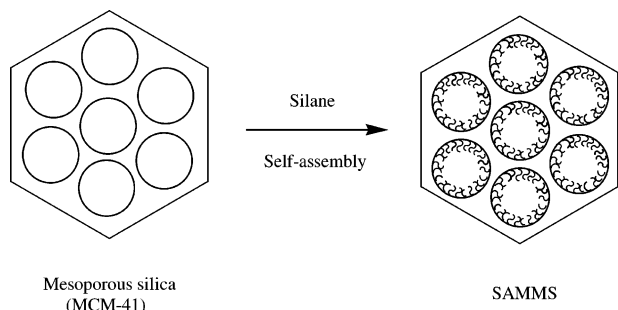
FIGURE 1. Preparation of SAMMS. By varying the interfacial ligand field of the monolayer, it is possible to tailor the SAMMS to sequester different classes of environmental contaminants.

perature under N_2 for at least 4 h. While the silane solution was being stirred, a sample of mesoporous silica (MCM-41 (29) with a surface area of 900 m^2/g and pore diameter of 60 Å) was suspended in toluene and treated with approximately 2 monolayers worth of water (0.31 mL of water for each gram of MCM-41). This suspension was then stirred for at least 2 h to make sure that the water was uniformly distributed throughout the mesoporous matrix. At the end of this pretreatment, an aliquot of the silane solution described

above was added to the MCM-41 suspension. Previous experience with silane monolayer chemistry indicated that no more than about 2 silanes/nm^2 would be incorporated into the monolayer with an aromatic headgroup (33). Thus, the amount of silane added was sufficient to meet this 2 silanes/nm^2 limit; this was later found to be justified when the population density of the HOPO ligands measured by solid-state ^{29}Si NMR was found to be approximately 0.5–1.0 silanes/nm^2. This solution was then taken to reflux for 6 h. After this period, it was cooled to ambient temperature, filtered, washed with 2-propanol, and air-dried.

Deprotection was accomplished by treating the benzylated SAMMS with 10% HBr in acetic acid and stirring the suspension overnight at ambient temperature. The product was collected by filtration, washed with 2-propanol, and air-dried. Removal of the benzyl protecting group was confirmed by solid-state ^{13}C NMR.

Batch Contacts with Actinide Solutions. All medium solutions were prepared from the reagent grade chemicals. For Pu(IV) adsorption experiments, concentrated HNO_3 was added into 0.1 or 1.0 M sodium nitrate solution to obtain 0.1 M acid concentration or titrated into the nitrate solution to reach pH 2. Aliquots of these solutions were spiked with ^{239}Pu(IV) to reach a nominal concentration of 2000 dpm/mL.
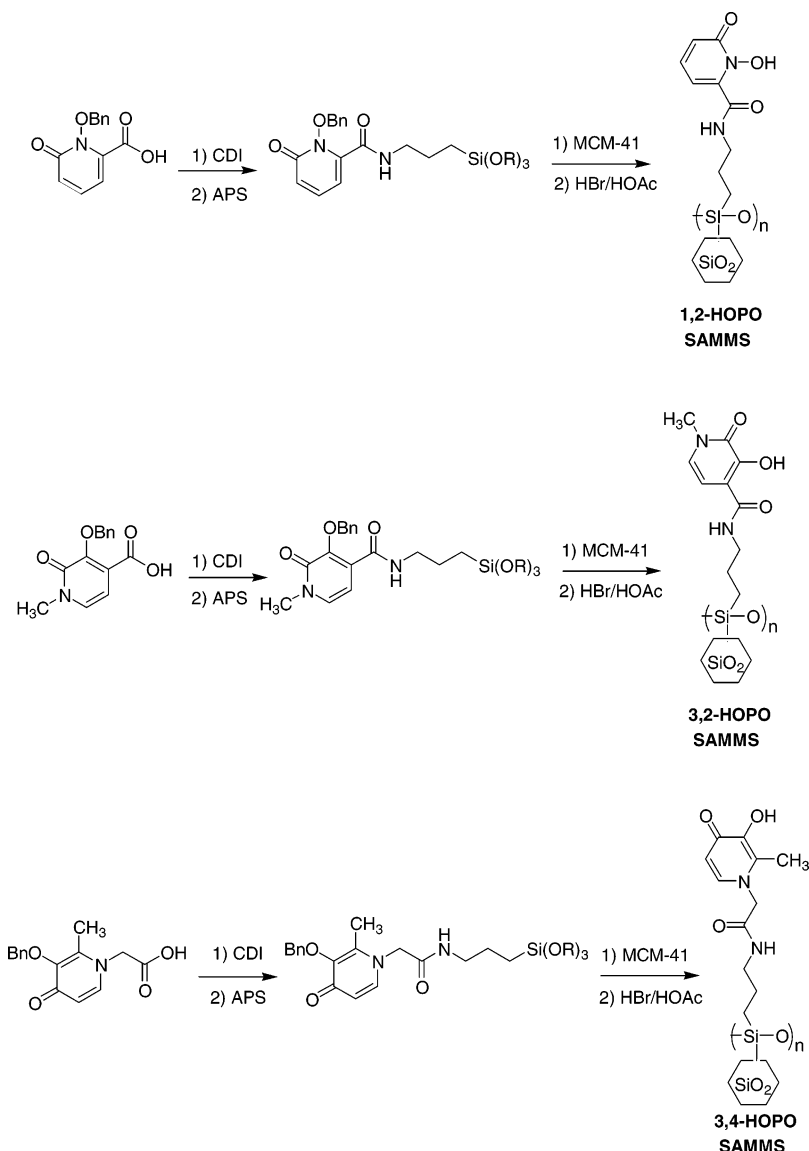
FIGURE 2. Synthesis of HOPO–SAMMS.

The stock [239]Pu was prepared in-house in 7 M HNO₃. For the interference study, the Pu(IV) solution was spiked with various ions using the ICP standard solutions (each comprised of 10 000 mg/L metal ion in 1–4% HNO₃, Aldrich Co). Then each SAMMS material was added into the prepared solution to obtain a liquid-to-solid ratio (L/S) of 200. The samples were shaken overnight in an orbital shaker. Then the aliquots were filtered through 0.2-μm syringe filters. The filtrates were subsequently suspended in Ultima Gold (Packard Instrument, Meriden, CT) scintillation cocktail, and the α activities were measured using a 2550 TR/AB liquid scintillation counter (Packard Instruments). With a 30-min count time, the detection limit was found to be 2.4 dpm/mL. The metal ion binding affinity is reported in term of the diffusion coefficient (K_d) which is defined as

$$K_d = \frac{(C_o - C_f)}{C_f} \frac{L}{S} \qquad (1)$$

where C_o and C_f are the initial and final metal ion concentrations in solution (mg/mL or dpm/mL), L is the solution volume (mL), and S is the mass of solid SAMMS (g).

The U(VI) adsorption experiments were performed in the same fashion of Pu(IV) adsorption. U(VI) solution was prepared by diluting the stock solution (350 μM U(VI) in 0.1 M HClO₄) in a required medium (i.e., nitrate, nitric acid, or nitrate/acetate mixture). The initial and final concentrations of U(VI) were measured by the Kinetic Phosphorescence Analyzer (KPA) (Chemchek Instruments, Inc., Richland, WA) having the lower detection limits of 0.1 μg/L.

Np(V) adsorption experiments were conducted by contacting samples of [237]Np-spiked groundwater and waste glass leachate (540–560 pCi/L) with known quantities of HOPO–SAMMS material. The solution-to-solid ratios in these experiments ranged from 100 to 10 000 mL/g. After 24 h of contact time, [237]Np activity in filtered aliquots were measured by γ-ray spectrometry, using a calibrated Wallac 1480 Wizard 3-in. NaI detector with built-in software. Samples were counted for a total of 10 000 counts. Limits of detection were 100 pCi.

Kinetics. Adsorption kinetics of Pu(IV) on 1,2-HOPO– and 3,2-HOPO–SAMMS were performed in the batch contact. The medium solution was 1.0 M NaNO₃/0.1M HNO₃. Each SAMMS was added to the solution to obtain the L/S ratio of 667. Sample aliquots were removed at the specified time intervals ranging from 1 min to 6 h. Each aliquot (about 1% of total volume) was removed, filtered through a 0.2-μm filter, and counted for α activities using the liquid scintillation. Samples were counted for 30 min.

Results and Discussions

The synthesis of HOPO SAMMS is outlined in Figure 2. The CDI-mediated silane coupling reaction was straightforward, and the deposition onto hydrated MCM-41 took place uneventfully. Analysis by solid-state ²⁹Si NMR revealed a functional density of approximately 0.5–1 silane/nm² (in accord with previous observations for aryl substituents in self-assembled monolayers; 33). Attempts to install the APS monolayer in the MCM-41 backbone first and then subsequently attach the CDI-activated HOPO ligands, while successful, did not work nearly as well as preforming the silane and then depositing. This is presumably due to the steric congestion that builds at the monolayer interface as the reaction progresses with the benzyl-protected HOPO ligands.

Pu(IV) Removal. Table 1 summarizes the distribution coefficients for Pu(IV), obtained from batch contact experiments with three HOPO–SAMMS materials. The initial Pu-(IV) was 2000 dpm/mL and L/S was 200. In acidic media, the

TABLE 1. Pu(IV) Distribution Coefficients on HOPO–SAMMS Materials[a]

medium	1,2-HOPO–SAMMS	3,2-HOPO–SAMMS	3,4-HOPO–SAMMS
0.1 M NaNO₃/0.1 M HNO₃	356 000	37 000	43 500
0.1 M NaNO₃ (pH 2.0)	349 000	350 000	17 500

[a] Initial Pu(IV) = 2000 dpm/mL, solution/solids = 200. Average of duplicate runs.
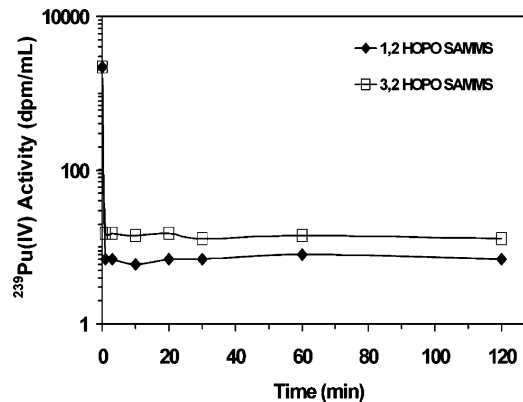
FIGURE 3. Pu(IV) sorption kinetics by 1,2- and 3,2-HOPO–SAMMS.

lower protonation constant of the chelating agent, the better the ligand affinity is. The lowest protonation constant among the three various HOPO ligands is found with 1,2-HOPO–SAMMS (2), which yielded the highest distribution coefficient for Pu(IV). A very important feature of the HOPO ligands is the strong hydrogen bond formed between the amide proton and the adjacent phenolic oxygen in the metal complex, thereby enhancing the stability of the complex (1). This feature stabilizes the 1,2-HOPO and the 3,2-HOPO adducts but is not available for the 3,4-HOPO complex. As a result, the 3,4-HOPO–SAMMS, which has the highest protonation constant and no intramolecular H-bond stabilization, yielded the lowest distribution coefficient of Pu(IV) of the HOPO SAMMS. The 3,2-HOPO–SAMMS with intermediate protonation constant adsorbed Pu(IV) well at 0.1 M NaNO₃ (pH 2.0), but the adsorption decreased by 10-fold as the acid concentration increased to 0.1 M.

The relatively close proximity of the HOPO ligands on the surface allows for multiple ligand–metal interactions once the actinide species is bound to the surface. NMR analysis reveals that the ligand population density is approximately 0.5–1 silane/nm². These silanes are approximately 1.2 nm long. Therefore, it is possible for two, three, and conceivably even four ligands to bind a single metal cation in these systems. The geometry of the Pu(IV) adduct is postulated to be 8-coordinate (either square prism or square anti-prism geometry), based in part on EXAFS analysis of a similar model system using the Eu adduct of salicylamide SAMMS (34). Interestingly, this model requires the interaction of four of the HOPO ligands with the Pu(IV) ion, suggesting a high degree of conformational flexibility within the monolayer interface.

Sorption Kinetics. Figure 3 shows the adsorption kinetics of Pu(IV) on 1,2-HOPO– and 3,2-HOPO–SAMMS at a solution-to-solids ratio of 667. The initial Pu(IV) concentration was 2200 dpm/mL (in 1.0 M NaNO₃/0.1 M HNO₃ solution). The Pu(IV) sorption was very rapid, with over 99% of the Pu(IV) being removed within the first minute (in both cases). This is similar to the kinetics displayed by other classes of SAMMS (15–19) and is due to the rigid, open-pore structure of SAMMS and the facile diffusion and open access to the ligand field allowed by this morphology.

TABLE 2. Competition Experiments with Pu(IV) and HOPO—SAMMS[a]

competitor	concn	1,2-HOPO—SAMMS	3,2-HOPO—SAMMS	3,4-HOPO—SAMMS
none		83 700	41 900	4 250
Fe(III)	100 ppm	17 800	30 700	495
Al(III)	100 ppm	28 400	27 700	5 370
Zr(IV)	100 ppm	417	47 300	63
Ni(II)	100 ppm	83 400	46 000	4 420
Ca(II)	100 ppm	96 100	42 900	4 380
Mn(II)	100 ppm	84 000	46 500	4 710
Mo(VII)	100 ppm	29 000	39 600	0
Cu(II)	100 ppm	30 200	38 750	4 710
Pb(II)	100 ppm	84 700	50 400	3 980
Cr(III)	100 ppm	75 900	43 100	4 380
Hg(II)	100 ppm	61 300	55 600	2 580
phosphate	0.01 M	129 000	48 300	2 880
sulfate	0.01 M	85 900	53 200	128
EDTA	0.01 M	188 000	60 000	2 960
citrate	0.01 M	180 000	58 300	1 480

[a] Initial Pu(IV) = 2000 dpm/mL in 1.0 M $NaNO_3$/0.1 M HNO_3, solution/solids = 200. Average of duplicate runs.

TABLE 3. U(VI) Distribution Coefficients on HOPO—SAMMS[a]

medium	1,2-HOPO—SAMMS	3,2-HOPO—SAMMS
0.05 M $NaNO_3$/0.05 NaAc (pH 6)	>1 980 000	>1 980 000
0.05 M $NaNO_3$/0.05 NaAc (pH 4)	>1 985 000	>1 980 000
0.1 M $NaNO_3$ (pH 2)	>1 975 000	11 200
0.2 M HNO_3	3 810	368

[a] Initial U(VI) = 1 mg/L, solution/solids = 200. Average of duplicate runs.

Competitive Adsorption of Pu(IV). Table 2 summarizes the distribution coefficients of Pu(IV) as the solutions were spiked with various interfering species. As might be expected, the 3,4-HOPO—SAMMS (the weakest HOPO ligand) experienced the greatest degree of competition from other ions. Its binding affinity for Pu(IV) was decreased significantly in the presences of Fe(III), Zr(IV), Mo(VII), and sulfate anion. However, both 1,2-HOPO— and 3,2-HOPO—SAMMS were relatively insensitive to the presence of competing species, the exception being Zr(IV), which had a severe impact on 1,2-HOPO—SAMMS's binding affinity for Pu(IV).

When the nitrate concentration was increased from 0.1 M (Table 1) to 1.0 M (Table 2), the affinity of 1,2-HOPO— and 3,4-HOPO—SAMMS for Pu(VI) was noted to decrease significantly as a result of the nitrate competition for Pu(IV). Pu(IV) is known to form strong complexes with nitrate anion (35). It is intriguing to note that phosphate, citrate, and EDTA seem to enhance the Pu(IV) binding affinity of 1,2-HOPO— and 3,2-HOPO—SAMMS, suggesting some sort of ligand synergy in the macromolecular chelation process. Not being affected by other common cations, anions (i.e., nitrate, sulfate, phosphate), and competing ligands (i.e., EDTA, citrate), the 3,2-HOPO—SAMMS is a very attractive Pu(IV) sequestrant. In highly acidic wastes or the wastes containing no Zr(IV), the 1,2-HOPO—SAMMS may also be a good choice.

U(VI) Removal. Table 3 summarizes the distribution coefficients of U(VI) after the batch contact experiments with 1,2-HOPO— and 3,2-HOPO—SAMMS materials. The initial U(VI) was 1.0 mg/L and solutions-to-solids ratio was 200. On the basis of the K_d values, in nitrate/acetate mixtures at pH 4 and 6, both 1,2-HOPO— and 3,2-HOPO—SAMMS materials were comparable in binding with U(VI). In more acidic media (0.1 M $NaNO_3$ (pH 2) and 0.2 M HNO_3), the U(VI) adsorption trend was similar to those obtained from Pu(IV) adsorption: the 1,2-HOPO—SAMMS had higher binding affinity for U(VI) than the 3,2-HOPO—SAMMS did.

TABLE 4. Distribution Coefficients (K_d, mL/g) for Np(V) Using HOPO—SAMMS[a]

| solution/solid ratio (mL/g)	1,2-HOPO	3,2-HOPO	3,4-HOPO
Solution Matrix: Hanford Groundwater			
100	19 800	27 800	
500	33 300	135 000	905
1000	14 000	153 000	882
5000	15 600	188 000	1520
10000	11 500	48 900	2020
Solution Matrix: Hanford Groundwater Equilibrated Waste Glass			
100	5 900	9 670	
500	6 830	27 700	217
1000	4 020	23 900	312
5000	2 310	26 300	388
10000	2 050	11 500	498

[a] Average of duplicate runs.

TABLE 5. Composition of the Hanford Groundwater Matrix and Glass Leachate Matrix Used for the Np Binding Studies

constituent	groundwater (mg/L)	glass leachate (mg/L)
pH (SU)	8.1	7.8
condition (mS/cm)	0.40	0.56
alkaline (as CO_3^{2-})	54.1	67.5
Cl	7.8	22.0
Br	0.10	<0.01
F	0.17	<0.01
I	<0.005	<0.005
NO_2^-	0.68	<0.01
NO_3^-	27.2	1.7
PO_4^{-3}	<0.01	0.3
SO_4^{-2}	82.5	108.0
Al	0.01	0.02
B	<0.05	0.11
Ba	<0.03	0.03
Be	<0.01	0.01
Ca	49.5	61.4
Fe	0.07	<0.05
K	1.7	8.3
Mg	14.6	16.1
Mn	0.17	0.03
Na	13.2	46.0
Si	16.5	16.6

The actinide AnO_2 complexes are known to have four, five, and six ligands in the equatorial plane (the O=U=O fragment is, of course, linear and defines the axis of the complex) (36). For the UO_2^{2+} adduct, we postulate that the equatorial region of the complex has two, and possibly three, HOPO ligands surrounding the uranyl moiety. In the case of the bis—HOPO adduct, this complex would be pseudo-octahedral. In the case of the tris—HOPO adduct, the complex would like hexagonal bipyramidal. Given the moderate reclining angle of the silane imposed by their spacing on the surface, this geometry is possible, but there may be slight puckering of the complex, resulting in more of a "propeller" geometry. Either binding scheme provides a strong binding affinity for sequestering the U(VI) species.

Np(V) Binding. NpO_2^+ is a more difficult species to bind (37). On the basis of the successful sequestration of Pu(IV) and U(VI) using HOPO—SAMMS, we chose to study the far more difficult target of sequestering Np(V). In our previous work (37), we were essentially unable to bind Np(V) using CMPO analogue ligands, and we felt that the HOPO ligands might offer some hope for effective sequestration of Np(V). In this case, to be more realistic for sequestering Np(V) released into the environment (either from leaking tanks or from glass leachate), these studies were carried out in a Hanford groundwater matrix at a pH of 7.8 (the composition of which is given in Table 5). Control experiments showed that NpO_2^+ was stable toward precipitation in this matrix. The solution-to-solids ratio was varied from 100 to 10 000.
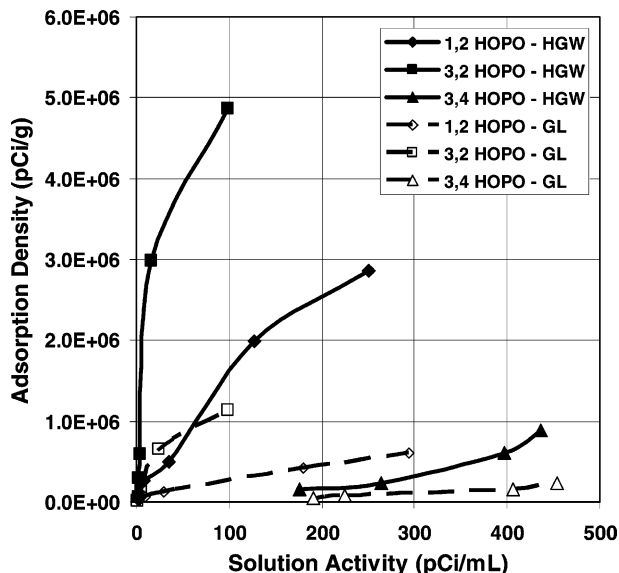
FIGURE 4. Np adsorption isotherms using HOPO−SAMMS and Hanford groundwater matrix and a simulated glass leachate matrix.

As can be seen from the data summarized in Table 4, all three of the HOPO−SAMMS were effective at binding Np(V) under these conditions, with the best performance being delivered by the 3,2-HOPO−SAMMS, with distribution coefficients as high as 188,000 being observed. Thus, the HOPO class of ligands has demonstrated exceptional capability for binding NpO_2^+ from a realistic environmental matrix.

Presenting the Np(V) sorption data in the form of absorption density as a function of solution concentration results in the plots summarized in Figure 4. As can be seen from these data, the efficiency of 1,2-HOPO− and 3,2-HOPO−SAMMS is considerably greater than that of 3,4-HOPO−SAMMS for removing Np(V) from a Hanford groundwater matrix, exactly as would be predicted based on the K_d values (Table 4). The 1,2-HOPO and 3,2-HOPO plots are not strictly linear, but they are still rising strongly at all levels studied. The plots for Np(V) using HOPO−SAMMS in a simulated glass leachate matrix were uniformly less efficient. The reason behind this attenuated performance is not entirely clear at this point. It is unlikely to be due to the modest shift in pH (8.2 vs 7.8) as these HOPO−SAMMS have shown excellent binding affinity for the actinides under far more acidic conditions (Tables 1−3), and there is very little competition from ubiquitous cations (e.g., Na, Ca, etc.) binding to the HOPO ligand (see Table 2). The possibility exists that some anion in the glass leachate matrix (e.g., carbonate, sulfate) is complexing the NpO_2^+ cation and having an impact on the ability of the HOPO−SAMMS to bind the complexed Np(V) species, but this hypothesis is still unconfirmed at this point.

Again, as with the UO_2^{2+} case discussed above, the NpO_2^+ ion is likely interacting with multiple HOPO ligands in these adducts. Molecular modeling studies, using the LANL2ZP ECP basis set, provided insight into why the 3,2-HOPO ligand has such high affinity for the NpO_2^+ ion. As shown in Figure 5, three 3,2-HOPO ligands surround the central NpO_2^+ species, with the upper and the lower HOPO ligands chelating the Np(V) cation. The middle HOPO ligand is bound to the Np(V) center in monodentate fashion, with bridging hydrogen bonds to the two neighboring HOPO ligands. The sixth equatorial coordination site on the NpO_2^+ ion is filled with a water molecule, shown at the 3 o'clock position in Figure 5. The multiple ligand−metal interactions as well as the intramolecular hydrogen bonding within the complexes provide additional driving force for sequestering the actinide cations within the HOPO monolayer.
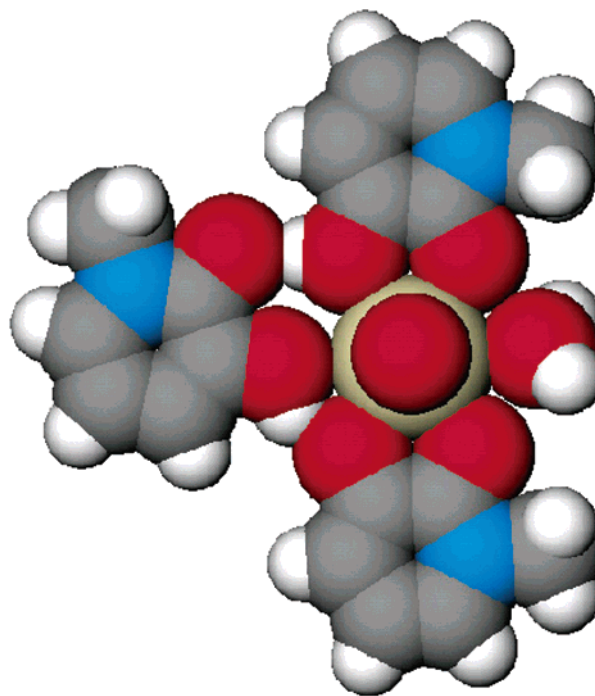
FIGURE 5. Structure suggested by molecular modeling (using LANL2ZP ECP basis set) of how the 3,2-HOPO ligand binds to NpO_2^+. Looking down the O−Np bond, the three HOPO ligands are seen surrounding the Np(V) ion (center). The upper and lower HOPO ligands are chelating the Np(V) ion, while the middle HOPO ligand is monodentate and has hydrogen bonds bridging to both the upper and lower ligands. The sixth equatorial site is occupied by a water molecule (shown on the right). (C atoms are gray, H atoms are white, N atoms are blue, O atoms are red, and the Np ion is brown).

In summary, incorporation of the HOPO class of ligands into the SAMMS environmental sorbent phases has resulted in a superior class of actinide sorbent materials. Multiple metal−ligand interactions are possible in these nanoporous sorbents, providing additional driving force for actinide binding. Sorption kinetics were found to be quite rapid (<1 min). Even the difficult to bind Np(V) was effectively scavenged, and in some cases Np(V) distribution coefficients exceeded 100 000.

Acknowledgments

Literature Cited

(1) Gorden, A. E. V.; Xu, J.; Raymond, K. N.; Durbin, P. W. Rational design of sequestering agents for plutonium and other actinides. *Chem. Rev.* **2003**, *103* (11), 4207−4282.

(2) Xu, J.; Whisenhunt, D. W., Jr.; Veeck, A. C.; Uhlir L. C.; Raymond, K, N. Thorium(IV) complexes of bidentate hydroxypyridinonates. *Inorg. Chem.* **2003**, *42*, 2665−2674.

(3) Xu, J.; Durbin, P. W.; Kullgren, B.; Ebbe, S. N.; Uhlir L. C.; Raymond, K. N. Synthesis and initial evaluation for in vivo chelation of Pu (IV) of a mixed octadentate spermine-based ligand containing 4-carbamoyl-3-hydroxy-1-methyl-2(1*H*)-pyridinone and 6-carbamoyl-1-hydroxy-2(1*H*)-pyridinone. *J. Med. Chem.* **2002**, *45*, 3963−3971.

(4) Xu, J.; Radkov, E.; Ziegler, M.; Raymond, K. N. Plutonium(IV) sequestration: Structural and thermodynamic evaluation of the extraordinarily stable cerium(IV) hydroxypyridinonate complexes. *Inorg. Chem.* **2000**, *39*, 4156−4164.

(5) Durbin, P. W.; Kullgren, B.; Xu, J.; Raymond, K. N.; Hengè-Napoli, M. H.; Bailly, T.; Burgada, R. Octadentate hydroxy-pyridinonate (HOPO) ligands for plutonium(IV): Pharmaco-kinetics and oral efficacy. *Radiat. Prot. Dosim.* **2003**, *105*, 503−508.

(6) Guilmette, R. A.; Hakimi, R.; Durbin, P. W.; Xu, J.; Raymond, K. N. Competitive binding of Pu and Am with bone mineral and novel chelating agents. *Radiat. Prot. Dosim.* **2003**, *105*, 527−534.

(7) White, D. L.; Durbin, P. W.; Jeung, N.; Raymond, K. N. Specific sequestering agents for the actinides. 16. Synthesis and initial biological testing of polydentate oxohydroxypyridinecarboxylate ligands. *J. Med. Chem.* **1988**, *31*, 11.

(8) Xu, J.; Kullgren, B.; Durbin, P. W.; Raymond, K. N. Specific sequestering agents for the actinides. 28. Synthesis and initial evaluation of multidentate 4-carbamoyl-3-hydroxy-l-methyl-2(l*H*)-pyridinone ligands for in vivo plutonium(IV) chelation. *J. Med. Chem.* **1995**, *38*, 2606.

(9) Xu, J. D.; Raymond, K. N. Uranyl sequestering agents: Cor-relation of properties and efficacy with structure for UO_2^{2+} complexes of linear tetradentate 1-methyl-3-hydroxy-2(1*H*)-pyridinone ligands. *Inorg. Chem.* **1999**, *38*, 308.

(10) Whisenhunt, D. W., Jr.; Neu, M. P.; Hou, Z.; Xu, J.; Hoffman, D. C.; Raymond, K. N. Specific sequestering agents for the actinides. 29. Stability of the thorium(IV) complexes of desferrioxamine B (DFO) and three octadentate catecholate or hydroxypyridi-nonate DFO derivatives: DFOMTA, DFOCAMC, and DFO-1,2-HOPO. Comparative stability of the plutonium(IV) DFOMTA Complex. *Inorg. Chem.* **1996**, *35*, 4128.

(11) Romanovski, V. V.; White, D. J.; Xu, J.; Hoffman, D. C.; Raymond, K. N. Plutonium(IV) and plutonium(VI) extraction by 1,2-hydroxypyridinone-6-*N*-octyl carboxamide. *Solvent Extr. Ion Exch.* **1999**, *17*, 55−71.

(12) Zhao, P. H.; Romanovski, V. V.; Whisenhunt, D. W.; Hoffman, D. C.; Mohs, T. R.; Xu, J. D.; Raymond, K. N. Extraction of plutonium by chelating hydroxypyridinone and catecholamide resins. *Solvent Extr. Ion Exch.* **1999**, *17*, 1327.

(13) Feng, X. D.; Fryxell, G. E.; Wang, L. Q.; Kim, A. Y.; Liu, J.; Kemner, K. Functionalized monolayers on mesoporous supports. *Science* **1997**, *276*, 923.

(14) Liu, J.; Feng, X.; Fryxell, G. E.; Wang, L. Q.; Kim, A. Y.; Gong, M. Hybrid mesoporous materials with functionalized monolayers. *Adv. Mater.* **1998**, *10*, 161−165.

(15) Chen, X.; Feng, X.; Liu, J.; Fryxell, G. E.; Gong, M. Mercury separation and immobilization using self-assembled monolayers on mesoporous supports (SAMMS). *Proceedings of the 10th Symposium on Separation Science and Technology for Energy Applications*, October 20−24, 1997; Gatlinburg, TN.

(16) Kemner, K.; Feng, X.; Liu, J.; Fryxell, G. E.; Wang, L.-Q.; Kim, A. Y.; Gong, M.; Mattigod, S. Investigation of the local chemical interactions between Hg and self-assembled monolayers on mesoporous supports. *J. Synchrotron Radiat.* **1999**, *6*, 633−635.

(17) Mattigod, S. V.; Feng, X.; Fryxell, G. E.; Liu, J.; Gong, M. Separation of complexed mercury from aqueous wastes using self-assembled mercaptan on mesoporous silica. *Sep. Sci. Technol.* **1999**, *34*, 2329−2345.

(18) Lin, Y.; Fryxell, G. E.; Wu, H.; Engelhard, M. Selective sorption of cesium using self-assembled monolayers on mesoporous supports (SAMMS). *Environ. Sci. Technol.* **2001**, *35*, 3962.

(19) Mattigod, S. V.; Fryxell, G. E.; Serne, R. J.; Parker, K. E.; Mann, F. M. Evaluation of novel getters for adsorption of radioiodine from groundwater and waste glass leachates. *Radiochim. Acta* **2003**, *91*, 539−545.

(20) Fryxell, G. E.; Lin, Y.; Wu, H.; Kemner, K. M. Environmental applications of self-assembled monolayers on mesoporous supports (SAMMS). In *Studies in Surface Science and Catalysis*, Vol. 141; Sayari, A., Jaroniec, M., Eds.; Elsevier: Amsterdam, 2003; pp 583−590.

(21) Yantasee, W.; Lin, Y.; Fryxell, G. E.; Wang, Z. Carbon paste electrode modified with carbamoylphosphonic acid function-alized mesoporous silica: A new mercury-free sensor for uranium(VI) detection. *Electroanalysis* **2004**, *16* (10), 870−873.

(22) Yantasee, W.; Lin, Y.; Fryxell, G. E.; Busche, B.; Birnbaum, J. C. Removal of heavy metals from aqueous solution using novel nanoengineered sorbents: Self-assembled carbamoylphos-phonic acids on mesoporous silica. *Sep. Sci. Technol.* **2003**, *38*, 3809−3825.

(23) Birnbaum, J. C.; Busche, B.; Lin, Y.; Shaw, W.; Fryxell, G. E. Synthesis of carbamoylphosphonate silanes for the selective sequestration of actinides. *Chem. Commun.* **2002**, *13*, 1374.

(24) Fryxell, G. E.; Liu, J.; Mattigod, S. V.; Wang, L. Q.; Gong, M.; Hauser, T. A.; Lin, Y.; Ferris, K. F.; Feng; X. Environmental applications of interfacially modified mesoporous ceramics. In *Ceramics Transactions, Vol. 107, Environmental Issues and Waste Management Technologies in the Ceramic and Nuclear Industries*; Chandler, G. T., Feng, X., Eds.; 2000; pp 29−37.

(25) Fryxell, G. E.; Liu, J.; Hauser, T. A.; Nie, Z.; Ferris, K. F.; Mattigod, S. V.; Feng, X.; Gong, M.; Hallen, R. T. Design and synthesis of selective mesoporous anion traps. *Chem. Mater.* **1999**, *11*, 2148.

(26) Kelly, S.; Kemner, K.; Fryxell, G. E.; Liu, J.; Mattigod, S. V.; Ferris, K. F. An X-ray absorption fine structure spectroscopy study of the interactions between contaminant tetrahedral anions to self-assembled monolayers on mesoporous supports. *J. Phys. Chem.* **2001**, *105*, 6337−6346.

(27) Yoshitake, H.; Yokoi, T.; Tatsumi, T. Adsorption of chromate and arsenate by amino-functionalized MCM-41 and SBA-1. *Chem. Mater.* **2002**, *14* (11), 4603−4610.

(28) Yoshitake, H.; Yokoi, T.; Tatsumi, T. Adsorption behavior of arsenate at transition metal cations captured by amino-functionalized mesoporous silicas. *Chem. Mater.* **2003**, *15* (8), 1713−1721.

(29) Kresge, C. T.; Leonowicz, M. E.; Roth, W. J.; Vartuli, J. C.; Beck, J. S. Ordered mesoporous molecular-sieves synthesized by a liquid-crystal template mechanism. *Nature* **1992**, *359*, 710.

(30) Fryxell, G. E.; Liu, J. Designing surface chemistry in mesoporous silica. In *Adsorption at Silica Surfaces*; Papirer, E., Ed.; Marcel Dekker: New York, 2000; pp 665−688.

(31) Moller, K.; Bein, T. Inclusion chemistry in periodic mesoporous hosts. *Chem. Mater.* **1998**, *10*, 2950−2963.

(32) Kontoghiorghes, G. J.; Sheppard, L. Simple synthesis of the potent iron chelators 1-alkyl-3-hydroxy-2-methylpyrid-4-ones. *Inorg. Chim. A-Biol.* **1987**, *136*, L11.

(33) Fryxell, G. E. unpublished NMR studies.

(34) Fryxell, G. E.; Wu, H.; Lin, Y.; Shaw, W. J.; Birnbaum, J. C.; Linehan, J. C.; Nie, Z.; Kemner, K. M.; Kelly, S. Lanthanide selective sorbents: Self-assembled monolayers on mesoporous supports (SAMMS). *J. Mater. Chem.* (in press).

(35) Cotton F. A.; Wilkinson, G. *Advanced Inorganic Chemistry*, 4th ed.; John Wiley and Sons: New York, 1980; pp 1017−1020.

(36) Cotton F. A.; Wilkinson, G. *Advanced Inorganic Chemistry*, 4th ed.; John Wiley and Sons: New York, 1980; p 1016.

(37) Fryxell, G. E.; Lin, Y.; Fiskum, S.; Birnbaum, J. C.; Wu, H.; Kemner, K. M.; Kelly, S. Actinide sequestration using self-assembled monolayers on mesoporous supports (SAMMS). *Environ. Sci. Technol.* Submitted for publication.